

Plant Succinic Semialdehyde Dehydrogenase: Dissection of Nucleotide Binding by Surface Plasmon Resonance and Fluorescence Spectroscopy[†]

Karin Busch,^{*,‡} Jacob Piehler,[§] and Hillel Fromm^{‡,||}

Departments of Plant Sciences and Biological Chemistry, The Weizmann Institute of Science, Rehovot 76100, Israel, and Centre for Plant Sciences, Leeds Institute for Biotechnology and Agriculture (LIBA), School of Biology, University of Leeds, Leeds LS2 9JT, U.K.

Received March 15, 2000

ABSTRACT: Recent kinetic studies revealed distinct modes of inhibition of mitochondrial *Arabidopsis thaliana* succinic semialdehyde dehydrogenase (*At*-SSADH1) by AMP and ATP. Inhibition of SSADH by ATP may represent an important mechanism of feedback regulation of the GABA shunt by the respiratory chain. Here we used two approaches to investigate the interaction of ATP with *At*-SSADH1. Cofactor displacement studies based on the reduced fluorescence intensity of free NADH versus that of enzyme-bound NADH revealed that both AMP and ATP decreased NADH–*At*-SSADH1 complex formation. The competitive inhibitor AMP displaced all bound NADH, while ATP, a noncompetitive inhibitor, could not, even in great excess, release all NADH from its binding site. To assess the effect of ATP on NAD–*At*-SSADH, we employed surface plasmon resonance to monitor nucleotide binding to immobilized *At*-SSADH1. For this, we used a Strep-tag II modified derivative of *At*-SSADH1 (designated ST-*At*-SSADH1). The tagged enzyme was tightly and reversibly captured by StrepTactin, which was covalently immobilized on a CM5 chip. The binding constants for NAD⁺ and ATP were determined from titration curves and were in good agreement with the constants obtained from enzyme kinetics. Surface plasmon resonance measurements confirmed that ATP binds to a site different from the binding site for NAD⁺. GTP competed with ATP. However, only ATP increased the dissociation constant of NAD⁺ from SSADH. This explains the reduced affinity of NAD⁺/NADH to *At*-SSADH1 in the presence of ATP, as revealed by enzymatic kinetics, and supports our model of feedback regulation of SSADH and the GABA shunt by ATP.

Succinic semialdehyde dehydrogenase (SSADH) is the last enzyme of the γ -aminobutyric acid (GABA) shunt, located at a junction between the GABA shunt, Krebs cycle, and respiratory chain. The GABA shunt is a bypass of the Krebs cycle between 2-oxoglutarate and succinate (1). Its exact role in plants is not clear. However, its proper regulation is essential for normal plant development (2). The first enzyme of the GABA shunt, glutamate decarboxylase (GAD), is a prominent calcium/calmodulin-binding protein in plants (2, 3) and is localized in the cytosol. The two other enzymes of the shunt, GABA transaminase and SSADH, are localized in mitochondria (4, 5). Recently, we cloned a cDNA encoding SSADH from *Arabidopsis thaliana* (*At*-SSADH1) and demonstrated that the recombinant enzyme functions as a homotetramer with distinct responses to different nucle-

otides. Analysis of *At*-SSADH1 enzymatic kinetics revealed its inhibition by NADH and adenine nucleotides, with K_I values between 120 μ M and 8 mM (5). The kinetic data suggested that AMP is a competitive inhibitor with respect to NAD⁺ binding, reflected in changing of the K_M for NAD⁺ but not the V_{max} . In contrast, ATP is a noncompetitive inhibitor with respect to NAD⁺, reflected in changing both the K_M and V_{max} of the enzyme (5). While the competitive effect of AMP has been known for several years (6) and can be explained by the high similarity between AMP and the adenine nucleotide part of NAD(H), the inhibitory effect of ATP has not been reported in other organisms. However, the noncompetitive effect of ATP on SSADH has interesting physiological implications. It signifies feedback regulation, since SSADH supplies the mitochondrial respiratory chain with two substrates, succinate and NADH, and the end product of the respiratory chain is ATP.

Although the K_I values of the nucleotides correspond to biologically relevant concentrations, the assessment of these transient low-affinity interactions with the enzyme is challenging. In this study, we detected different modes of cofactor (NADH) displacement by various nucleotides by monitoring the fluorescence of NADH. Furthermore, we established mass-sensitive detection of nucleotide–enzyme interactions by surface plasmon resonance (SPR). In this assay, the

[†] K.B. was the recipient of a MINERVA postdoctoral fellowship from 1997 to 1999. J.P. was an EMBO postdoctoral fellow, 1998–1999.

* Corresponding author. Current address: Max-Planck-Institut für Entwicklungsbiologie, JRG-Schuster, Spemannstrasse 39, D-72076 Tübingen, Germany. Phone: x49-7071-601-482. Fax: x49-7071-601-442. E-mail: karinb@oeserverg3.biochem.mpg.de.

[‡] Department of Plant Sciences, The Weizmann Institute of Science.

[§] Department of Biological Chemistry, The Weizmann Institute of Science.

^{||} University of Leeds.

enzyme was affinity captured, and the binding of different nucleotides, separately or in combination, was monitored by surface plasmon resonance.

EXPERIMENTAL PROCEDURES

Preparation of an N-Terminal Strep-tag of At-SSADH1. The StrepTactin-binding peptide Strep-tag II [WSHPQFEK (7); IBA, Goettingen, FRG) was added to the recombinant At-SSADH1 by extending the cDNA as follows. Two oligonucleotides with 5'-NcoI compatible protruding ends were annealed and ligated into the NcoI site of the linearized At-SSADH1 cDNA in the *Escherichia coli* expression vector pET-3d (5). The two oligonucleotides were (sense) 5'-CATGTGGAGCCATCCGCAATTTGAAAAAGC and (antisense) 5'-CATGGCTTTTTCAAATTGCGGATGGCTC-CA. Ten amino acids were added to At-SSADH1, and the N-terminus of the modified recombinant protein had the amino acid sequence: **MWSHPQFEKAMDAQSVS...** (the eight amino acid Strep-tag is in bold).

Expression and Purification of Recombinant Enzymes. At-SSADH1 was purified from *E. coli* by consecutive FPLC chromatographies on ion-exchange Q-Sepharose, Sephadex G-200 (16/60) gel filtration, and Blue Sepharose 6 Fast-Flow affinity (1.6/4) as described (5), except that the ammonium sulfate precipitation step was omitted. The active fractions resulting from the ion-exchange chromatography were directly loaded onto the gel filtration column. Expression of ST-At-SSADH1 was initiated by adding 0.5 mM isopropyl thio- β -D-galactoside to a 0.5 L cell culture in 2-YT medium for 7 h at 37 °C. Cells were broken in 10–15 mL buffer WP₁¹ containing 100 mM sodium phosphate, pH 9.0, 1 mM dithiothreitol (DTT), and 1 mM EDTA. After addition of 1 mM phenylmethanesulfonyl fluoride by sonication for 5 min at 0 °C, cell debris and insoluble protein were removed by centrifugation at 13 000 rpm for 20 min (Sorvall centrifuge, SS34 rotor). The recombinant protein was purified on a 1 mL StrepTactin affinity column according to the manufacturer's recommendations (IBA, Goettingen, FRG) by gravity flow. The supernatant containing soluble ST-At-SSADH1 was dialyzed against buffer WP_i, filtered, and loaded onto the column. Bound ST-At-SSADH1 was eluted by adding 6 \times 0.5 mL of buffer WP_i containing 2.5 mM desthiobiotin (Sigma) as a reversibly binding specific competitor. The active fractions were pooled, exhaustively dialyzed against buffer WP_i to remove desthiobiotin, and analyzed by SDS-PAGE. The recombinant enzyme accounted for ~10% of the total soluble protein, and typically 2–4 mg of purified enzyme with a homogeneity of >95% was obtained from 0.5 L of a bacterial culture. This grade of purity was sufficient for the affinity capturing. The purified ST-At-SSADH1 was enzymatically active, and the kinetic constants ($K_{0.5\text{SSA}} = 4.9 \mu\text{M}$ and $K_{\text{MNAD}} = 70 \mu\text{M}$) were determined by the activity assay described earlier (5). The kinetic constants were in the same range as those of At-SSADH1; thus, the additional 10 amino acid residues had no apparent effect on the enzymatic activity.

Fluorescence Spectroscopy and Enzyme Assay. Fluorescence measurements were performed in an SLM 8000C

instrument (SLM instruments, Urbana, IL) equipped with a xenon lamp (450 W) and an emission quartz prism monochromator (type MC640, double). The bandwidth for excitation was 16 nm. The excitation wavelength was 340 nm to monitor NADH, and the range for spectra acquisition was 380–500 nm. Measurements were done in 1 mL fluorescence cuvettes in 100 mM sodium phosphate buffer, pH 9.0, 10 mM MgCl₂, 10 mM sodium phosphate, and 1 mM DTT at 20 °C. Controls included NADH and inhibitors in the absence of enzyme.

Surface Plasmon Resonance Measurements. Nucleotide binding to ST-At-SSADH1 was monitored by surface plasmon resonance with a BIACORE 2000 apparatus (Biacore AB, SE). StrepTactin, a streptavidin mutant with improved affinity toward Strep-tag, was immobilized on a CM5 chip (Biacore AB, SE) by amine coupling chemistry using standard protocols with HBS (10 mM HEPES with 0.15 M NaCl, 3.4 mM EDTA, and 0.005% surfactant P20 at pH 7.4) as a running buffer. After activation with a freshly prepared mixture of *N*-hydroxysuccinimide (NHS, 50 mM in water) and 1-ethyl-3-(3-dimethylaminopropyl)carbodiimide (EDC, 200 mM in water) for 4 min, StrepTactin (50–200 $\mu\text{g mL}^{-1}$ in 20 mM acetate buffer, pH 4.6) was injected for 8–20 min (flow rate: 5 $\mu\text{L min}^{-1}$). Remaining activated carboxylic groups were deactivated by incubation with 1 M ethanolamine hydrochloride, pH 8.6, for 4 min (flow rate: 5 $\mu\text{L min}^{-1}$). A total of 5000–15 000 RU of StrepTactin were immobilized by this method. After coupling, the buffer was changed to 100 mM sodium phosphate, pH 9.0, 1 mM DTT, 10 mM MgCl₂, 10 mM potassium phosphate, and 0.005% surfactant P20, which was used throughout binding experiments. ST-At-SSADH1 (5 μM) (flow rate: 5 $\mu\text{L min}^{-1}$) was immobilized by affinity capturing with StrepTactin. Nucleotide binding was investigated by incubation at different concentrations for 1 min with a flow rate of 10 $\mu\text{L min}^{-1}$. As a reference, binding experiments were performed in parallel on a StrepTactin-coated sensor chip without ST-At-SSADH1. Other controls are described in the Results section.

Calculation of Binary Enzyme–Effector (Inhibitor) Complexes. The equilibrium effector (inhibitor) constant K_D of an enzyme–effector (inhibitor) complex is given by the concentration of the enzyme–effector (inhibitor) complex c_{EI} , the total enzyme concentration c_E , and the total effector (inhibitor) concentration c_I according to the law of mass action:

$$K_D = \frac{(c_E - c_{\text{EI}})(c_I - c_{\text{EI}})}{c_{\text{EI}}} \quad (1)$$

c_{EI} can be calculated from c_E and c_I for given effector constants according to

$$c_{\text{EI}} = \frac{c_E + c_I + K_D}{2} - \sqrt{\frac{(c_E + c_I + K_D)^2}{4} - c_E c_I} \quad (2)$$

At pseudo-first-order conditions in a flow-through system (constant c_I), c_{EI} as measured as a binding signal is given by

$$c_{\text{EI}} = c_{\text{E}1} \frac{c_I/K_D}{1 + c_I/K_D} \quad (3)$$

¹ Abbreviations: AU, arbitrary units; HABA, 2-(4'-hydroxybenzenazo)benzoic acid; HBS, HEPES-buffered saline; P_i, inorganic phosphate; RU, response units; SPR, surface plasmon resonance.

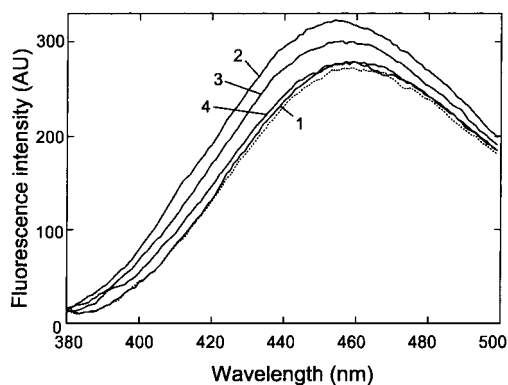


FIGURE 1: Competitive effect of AMP on the binding of NADH to *At*-SSADH1. Fluorescence spectra of (1) NADH (50 μ M), (2) NADH (50 μ M) + enzyme (20 μ M), (3) NADH (50 μ M) + enzyme (20 μ M) + AMP (5 mM), and (4) NADH (50 μ M) + enzyme (20 μ M) + AMP (25 mM) and a control spectrum (dotted line) of NADH (50 μ M) + AMP (25 mM).

To determine the dissociation constant K_D , titration curves resulting from the titration of captured ST-SSADH by increasing amounts of nucleotides were fitted according to the equation:

$$y = R_{\text{off}} + R_{\text{max}} \frac{c_1/K_D}{1 + c_1/K_D} \quad (4)$$

with the background signal R_{off} , the maximum signals R_{max} , and the dissociation constant K_D .

RESULTS

Fluorescence Measurements of Cofactor Displacement Distinguish between Competitive and Noncompetitive Inhibitors. We tested the feasibility of a few approaches to monitor nucleotide binding to SSADH by label-free methods. Monitoring ATP binding to *At*-SSADH1 by quenching of intrinsic tryptophan fluorescence was not possible, since addition of ATP hardly affected intrinsic fluorescence (excitation wavelength 295 nm, emission wavelength 330 nm; data not shown). Instead, we measured cofactor binding to *At*-SSADH1 by fluorescence emission spectroscopy. The fluorescent NADH is a competitive analogue of NAD^+ at the NAD^+ binding site of SSADH (5, 8). The binding of NADH to the enzyme is accompanied by an enhancement of the fluorescence emitted over the spectral range of 380–500 nm with a peak at 460 nm after excitation at 340 nm. In Figure 1 the fluorescence of free NADH (line 1) and enzyme-bound NADH (line 2) is shown. Subsequently, the dependence of the fluorescence intensity on the binding state of NADH was used to monitor the influence of different nucleotide inhibitors on cofactor binding to *At*-SSADH1.

AMP, a competitive inhibitor of *At*-SSADH1 with respect to NAD^+ and NADH (5), was expected to completely release NADH from the NAD^+ /NADH binding site in *At*-SSADH1 when added in excess. At 5 mM AMP, NADH fluorescence decreased (Figure 1, line 3) but was still higher than that of free NADH (Figure 1, line 1). At 25 mM AMP (Figure 1, line 4), the fluorescence intensity of NADH was identical to that of free NADH (line 1). The high AMP concentration was necessary due to the high K_I value in the millimolar range (Table 1, eq 2).

Table 1: Kinetic Constants and Mode of Action of Nucleotide Inhibitors of *At*-SSADH1

nucleotide	kinetic constant	value ^a (μ M)	type of inhibition	K_D (μ M)
NAD^+	K_M	130 ± 80	substrate	135 ± 60
NADH	K_I	120 ± 90	competitive	nd ^b
AMP	K_I	2900	competitive	nd
ATP	K_{IC}	2500	noncompetitive	4300 ± 600
	K_{IU}	8000		

^a Source: ref 5. ^b nd = not determined.

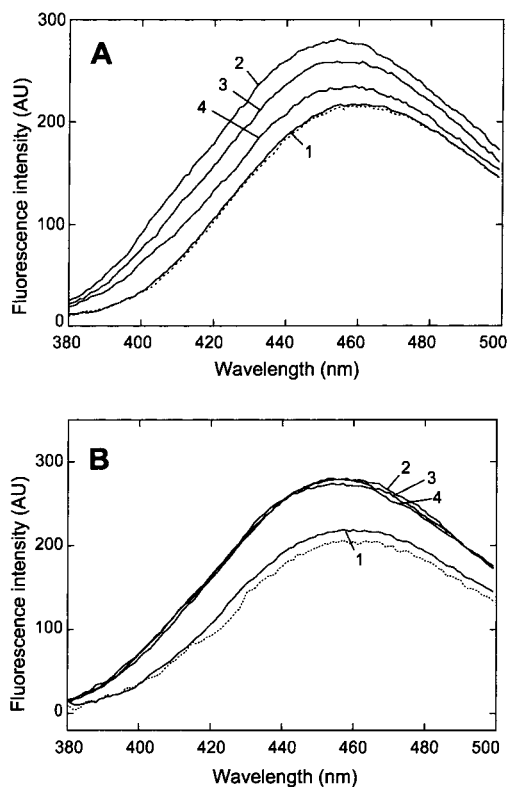


FIGURE 2: (A) Effect of ATP on the binding of NADH to *At*-SSADH1. Fluorescence spectra of (1) NADH (50 μ M), (2) NADH (50 μ M) + enzyme (20 μ M), (3) NADH (50 μ M) + enzyme (20 μ M) + ATP (5 mM), and (4) NADH (50 μ M) + enzyme (20 μ M) + ATP (25 mM) and a control spectrum (dotted line) of NADH (50 μ M) + ATP (25 mM). (B) Addition of GTP to the NADH–*At*-SSADH1 complex. Fluorescence spectra of (1) NADH (50 μ M), (2) NADH (50 μ M) + enzyme (20 μ M), (3) NADH (50 μ M) + enzyme (20 μ M) + GTP (5 mM), and (4) NADH (50 μ M) + enzyme (20 μ M) + GTP (25 mM) and a control spectrum (dotted line) of NADH (50 μ M) + GTP (25 mM) without enzyme.

Addition of ATP to NADH–*At*-SSADH1 lowered NADH fluorescence (Figure 2A, lines 3 and 4, corresponding to 5 and 25 mM ATP, respectively) in comparison to NADH bound to *At*-SSADH1 (line 2), indicating the release of NADH from the NAD^+ /NADH binding site. However, even at extremely high ATP concentrations (100 mM ATP; data not shown), NADH fluorescence intensity was not reduced to that of free NADH (line 1), indicating that not all bound NADH was released in the presence of ATP. This can be explained if ATP does not bind to the site occupied by NADH and does not substitute NADH directly but only influences the binding of the cofactor to the enzyme. Due to its high K_I (Table 1), ATP had to be in the millimolar range to bind in a sufficient amount to release NADH from the NAD^+ binding site (eq 2). In a control experiment, GTP,

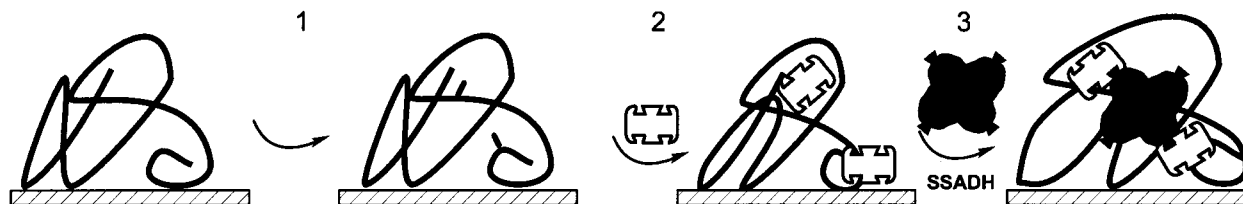


FIGURE 3: Schematic illustration of SSADH capturing on a StrepTactin-coated surface: (1) activation of the surface; (2) covalent immobilization of StrepTactin; (3) reversible immobilization of the tetrameric ST-*At*-SSADH1 by affinity capturing.

which has no effect on *At*-SSADH1 activity (data not shown), was added to the NADH-*At*-SSADH1 complex. As expected, GTP had no effect on NADH fluorescence. The fluorescence was the same in the absence and presence of 5 and 25 mM GTP, respectively (Figure 2B, lines 3 and 4, respectively). Thus, this fluorescence assay was found suitable as a rapid and qualitative means to demonstrate nucleotide interaction with *At*-SSADH1 and to assess the type of interaction.

Monitoring Protein–Nucleotide Interactions by Surface Plasmon Resonance (SPR). We employed SPR measurement in a BIACORE apparatus to directly measure binding of nucleotides to *At*-SSADH1. To assess direct binding of nonaltered nucleotides to the protein, we immobilized the enzyme rather than the nucleotides. Effects on structure and activity of the enzyme upon immobilization were minimized by reversible affinity capturing. For this, we prepared an N-terminal Strep-tag version of the recombinant enzyme (designated ST-*At*-SSADH1) by adding the corresponding codons to the cDNA (Experimental Procedures). The protein was purified by affinity chromatography and then captured onto a StrepTactin-coated chip surface, as schematically depicted in Figure 3, thus avoiding denaturation of the enzyme by the oxidative environment required for covalent coupling. Figure 4A shows an SPR sensorgram for capturing of ST-*At*-SSADH1 with immobilized StrepTactin. Depending on the amount of immobilized StrepTactin, 2500–6000 RU of ST-*At*-SSADH1 were captured. Immobilization of ST-*At*-SSADH1 by this method was perfectly reversible. Upon addition of 40 μ L of 10 mM desthiobiotin, ST-*At*-SSADH1 was completely released from the chip surface as shown in Figure 4B, and fresh ST-*At*-SSADH1 could be captured on the regenerated surface. After the surface was saturated with ST-*At*-SSADH1, the surface was washed with running buffer to remove weakly bound ST-*At*-SSADH1. With high amounts of immobilized StrepTactin (10 000–15 000 RU), little dissociation of ST-*At*-SSADH1 was observed. Probably most of the tetrameric ST-*At*-SSADH1 binds with more than one Strep-tag to the StrepTactin, and only proteins attached with a single tag were washed out. With increasing amounts of immobilized StrepTactin, multiple interactions with ST-*At*-SSADH1 were facilitated. As expected, the attachment of Strep-tag II to immobilized StrepTactin was more stable than that reported for Strep-tag I to immobilized streptavidin (9). Further nucleotide binding experiments were performed under conditions where dissociation of ST-*At*-SSADH1 from the surface was negligible.

When NAD⁺ was passed over ST-*At*-SSADH1 captured by immobilized StrepTactin, a significant fast increase in the refractive index was detected (Figure 5A, continuous line). Also, the reference surface (only StrepTactin) showed an increase in the signal due to the change in the refractive

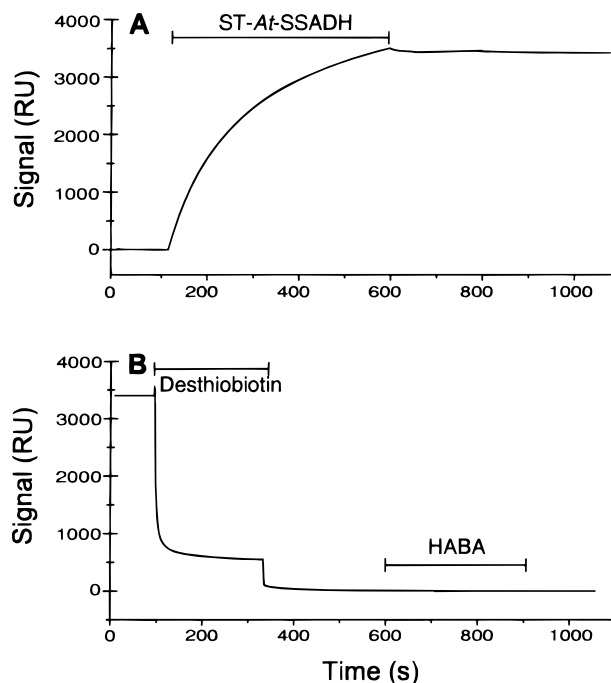


FIGURE 4: Immobilization of ST-*At*-SSADH1 by capturing with immobilized StrepTactin monitored by SPR. (A) Sensorgram for binding of ST-*At*-SSADH1 (5 μ M at 5 μ L min⁻¹) to StrepTactin. (B) Removal of ST-*At*-SSADH1 by injection of 10 mM desthiobiotin in the running buffer for 4 min (flow rate: 10 μ L min⁻¹).

index in the sample (Figure 5A, dotted line). However, a clearly stronger signal is observed on the channel with captured ST-*At*-SSADH1. Furthermore, the washout on this channel is much slower, indicating interaction of the nucleotide with the ST-*At*-SSADH1. Figure 5B shows the difference sensorgrams of the flow channels with and without captured ST-*At*-SSADH1 at different NAD⁺ concentrations. The intensity of the referenced signal was dependent on the NAD⁺ concentration. This concentration-dependent increase was reproducible on different channels, and with various loadings of StrepTactin and ST-*At*-SSADH1, indicating that specific nucleotide binding was detected. The dissociation constant of the NAD-*At*-SSADH1 complex was determined from the concentration dependence of the binding-dependent resonance signal by fitting eq 4 (Figure 6A). The calculated dissociation constant K_D was $135 \pm 60 \mu$ M, in excellent agreement with the K_I determined from enzyme kinetics [$K_M = 130 \pm 80 \mu$ M (5)]. The maximum amplitude of NAD⁺ binding was 25–40 RU, depending on the amount of captured ST-*At*-SSADH1. To further test the specificity of the resonance signal originating from nucleotide binding to ST-*At*-SSADH1, a reference chip with a different non-relevant protein (IgG), which does not bind nucleotides, was covalently immobilized to a similar amount (as StrepTactin plus ST-SSADH1). No significant signal was observed upon

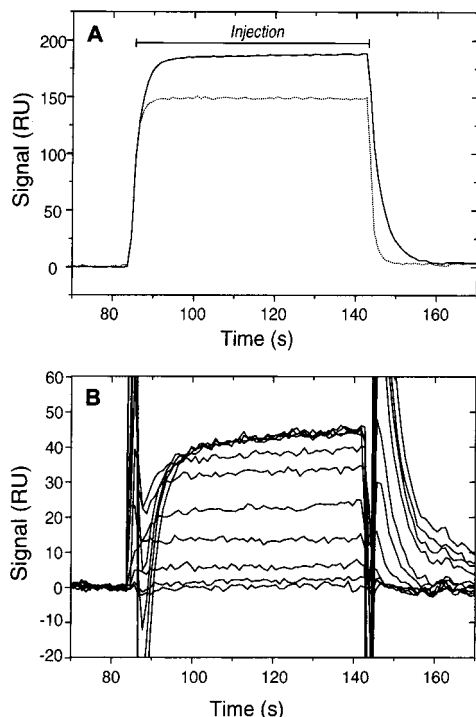


FIGURE 5: Surface plasmon resonance signals of NAD^+ binding to ST-*At*-SSADH1 for a 1 min pulse (injected with $10 \mu\text{L min}^{-1}$). (A) Sensorgram (StrepTactin-coated surface with captured ST-*At*-SSADH1) (continuous line) and a reference sensorgram (only StrepTactin) (dotted line) with injections of 1 mM NAD^+ . The sensorgram is a representative of three independent experiments. (B) Difference sensorgrams of the same titration experiment with injections of NAD^+ between 0.001 and 10 mM.

injection of NAD^+ , in comparison to measurements from a StrepTactin-coated pad without ST-*At*-SSADH1 (not shown). This confirmed that specific nucleotide binding to ST-*At*-SSADH1 was detected by this method. Thereafter, we used the StrepTactin-coated sensor chip without ST-*At*-SSADH1 as the reference.

ATP Enhances NAD^+ Dissociation from SSADH. Having established a method for direct measurement of nucleotide binding to SSADH, we examined ATP binding by injecting different concentrations of the nucleotide on StrepTactin-captured ST-*At*-SSADH1 and monitoring mass changes by surface plasmon resonance. Figure 6B shows the titration curve after injection of increasing concentrations of ATP. A concentration-dependent increase in the binding signal was measured up to 30 mM ATP. At ATP concentrations higher than 30 mM, however, the background signal became too high (>1000 RU) to quantify the subtle binding effects. Furthermore, dissociation of ST-*At*-SSADH1 from the chip was observed at these high concentrations. From the partial titration curve with ATP concentrations of up to 30 mM, a dissociation constant (K_D) of 4.3 mM was estimated for ATP binding to ST-*At*-SSADH1. A similar binding effect was observed in a control experiment with GTP, indicating that both nucleotides bind to ST-*At*-SSADH1 (not shown). However, only ATP had an influence on NAD^+ binding, as will be shown.

The influence of ATP and GTP on the NAD^+ -ST-*At*-SSADH1 interaction was investigated by measuring the dissociation constant of the NAD -ST-*At*-SSADH1 complex at different background concentrations of ATP and GTP. Concentrations of 2 and 5 mM ATP were chosen, which

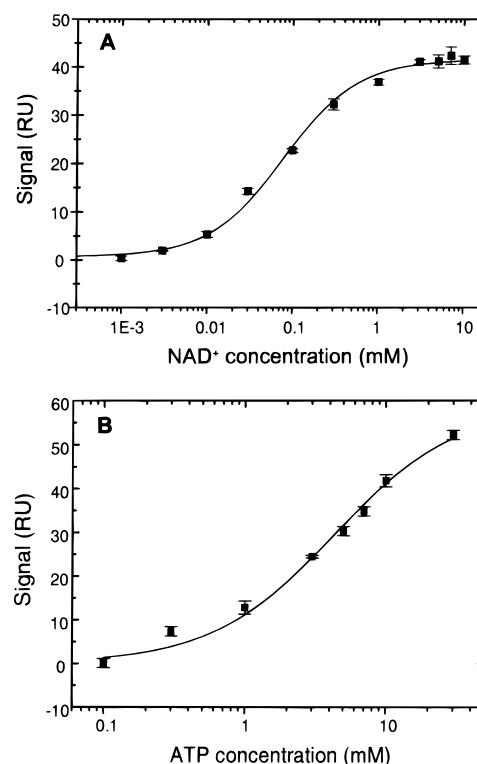


FIGURE 6: Titration of ST-*At*-SSADH1 with different nucleotides showing difference equilibrium SPR responses. (A) Titration of ST-*At*-SSADH1 with NAD^+ . The points represent the individual responses after 1 min pulse injections of increasing amounts of NAD^+ in the range of 0.001–10 mM NAD^+ at a flow rate of $10 \mu\text{L min}^{-1}$. Error bars show standard deviations for the means of three independent experiments. (B) Difference surface plasmon resonance signals corresponding to ST-*At*-SSADH1 titration with increasing concentrations of ATP. Increasing concentrations in the range of 0.1–30 mM ATP were injected at a flow rate of $10 \mu\text{L min}^{-1}$ in a 1 min pulse across a StrepTactin-coated surface with captured St-*At*-SSADH1. Error bars show standard deviations for the means of three independent experiments, respectively.

are in the biologically relevant range, and of 5 mM GTP for comparison. In these binding experiments, additional binding of ATP caused a constant background signal of 9 and 15 RU, respectively, while the amplitude of NAD^+ binding did not change significantly (shown in Figure 7A for 5 mM ATP). These results indicate that a different binding site is recruited by ATP as predicted by the displacement fluorescence assay described above. The dissociation constant of NAD^+ binding to SSADH at the different ATP background concentrations was determined by using eq 4. A significant increase compared to NAD^+ without ATP was observed, with a $K_D = 630 \pm 80 \mu\text{M}$ in the presence of 2 mM ATP and $K_D = 1100 \pm 30 \mu\text{M}$ in the presence of 5 mM ATP (Figure 7B). For NAD^+ binding with a background of 5 mM GTP, similar additive binding as for ATP was observed, indicating that GTP also binds to an alternative binding site. However, the K_D of NAD^+ binding was not affected at a GTP concentration of 5 mM (Figure 7B), in agreement with the results from the NADH displacement fluorescence assay and kinetic data (not shown). To assess whether both ATP and GTP recruit the same binding site, titration with ATP was carried out with and without a background of 10 mM GTP (Figure 8). The total binding amplitude did not change significantly, confirming that GTP binds competitively to the ATP binding site

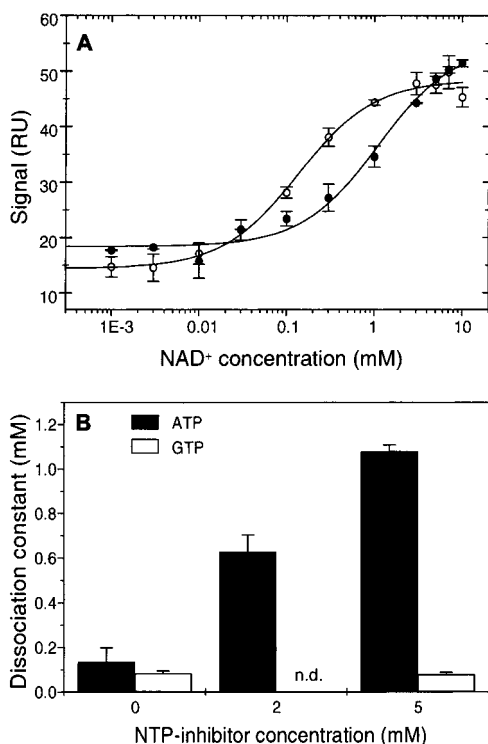


FIGURE 7: Influence of ATP and GTP on NAD⁺ binding to ST-*At*-SSADH1. (A) Titration of ST-*At*-SSADH1 with increasing amounts of NAD⁺ in the presence of constant 5 mM ATP (●) or GTP (○). The points represent the individual responses after 1 min pulse injections of increasing amounts of NAD⁺ in the range of 0.001–10 mM NAD⁺ at a flow rate of 10 μ L min⁻¹. Error bars show mean deviations for a set of three independent experiments. The lines result from fitting the data points by applying eq 4. (B) Dissociation constant K_D of the affinity-captured NAD–ST-*At*-SSADH1 complex on a StrepTactin-coated surface in the presence of different ATP concentrations (0, 2, and 5 mM) and 5 mM GTP. The K_D values were determined from titration curves by applying eq 4. The values are the means of three independent experiments. n.d.: not determined.

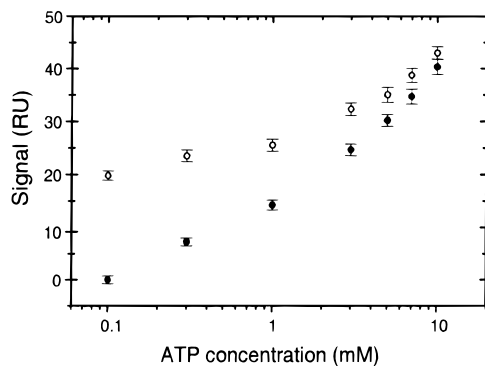


FIGURE 8: Titration of ST-*At*-SSADH1 with ATP in the absence (●) and presence of 10 mM GTP (○). The points represent corrected equilibrium SPR responses.

DISCUSSION

Recent kinetic studies revealed that ATP is a noncompetitive inhibitor of plant SSADH, a property that has not been reported for SSADH from any other organism. Mitochondrial SSADH is the last enzyme of the GABA shunt, which provides succinate and NADH as substrates for the respiratory chain. Inhibition of SSADH by ATP signifies a feedback regulation, since the end product of the oxidative phosphorylation is ATP. To assess this model, we attempted to

demonstrate ATP binding to *At*-SSADH1 and to reveal the mechanism underlying SSADH inhibition by ATP. The K_I values for ATP interactions with *At*-SSADH1 were in the millimolar range (5), indicating transient, low-affinity interaction. Weak nucleotide binding to proteins is difficult to monitor (10), and high concentrations of either the protein or the nucleotide are required to detect complex formation in such cases. In addition, certain approaches require the use of altered nucleotides such as fluorophore-labeled nucleotides for fluorescence measurement or biotinylated nucleotides for immobilization. These alterations substantially change the molecular entity in ways that might affect their interaction with the enzyme.

Evidence for ATP binding to *At*-SSADH1 and its mechanism of inhibition resulted from measuring the influence of ATP and AMP on cofactor (NADH) binding to *At*-SSADH1 by a fluorescence assay. The presence of the inhibitory nucleotide resulted in changes in NADH fluorescence by releasing it from the NAD⁺/NADH binding site. This revealed that, although ATP reduced the amount of the NAD–*At*-SSADH1 complex, it did not prevent its formation completely, even in great molar excess. Therefore, we excluded the possibility that displacement of NADH results from ATP binding at the cofactor binding site, indicating an additional binding site for ATP. With this fluorescence assay it was possible to distinguish between competitive and noncompetitive types of inhibition, as demonstrated for AMP and ATP, respectively.

We were able to measure binding of NAD⁺ and ATP to *At*-SSADH1 directly by surface plasmon resonance. This method required immobilization of either of the interacting compounds. To avoid modification of the nucleotide, we devised a strategy for a mild, reversible immobilization of SSADH by affinity capturing. ST-*At*-SSADH1 with the eight amino acid residue Strep-tag at the N-terminus was captured on a StrepTactin-coated surface. Thus, reducing conditions were maintained throughout all experiments with SSADH, guaranteeing maximal activity of the enzyme. The capturing was reversible so that the sensitive ST-*At*-SSADH1 could easily be renewed with freshly prepared protein, and the StrepTactin-coated chip was reusable for many times. The capturing of ST-*At*-SSADH1 was stable, as a result of the high affinity of the Strep-tag to StrepTactin but probably also because the tetrameric structure of the enzyme allows multiple interactions with StrepTactin. The high density of binding sites in the StrepTactin (one per subunit of 15 kDa), the specificity of the interaction, and the mild conditions for regeneration make this system advantageous over other protein tags. The frequently used His-tag, for example, does not provide this high selectivity, and it requires a highly loaded metal–chelator matrix for immobilization, which is prone to nonspecific interactions.

Binding of NAD⁺ (663 g/mol) confirmed the K_D of 135 μ M obtained from enzyme kinetics. Comparison of the maximum binding amplitude of NAD⁺ at different levels of captured ST-*At*-SSADH1 (3500–6000 RU) suggests a binding stoichiometry of \sim 0.5 nucleotide per subunit (53 kDa) or 2 NAD⁺ per SSADH tetramer. This is in good agreement with the stoichiometry of 2 NADH per SSADH tetramer earlier proposed for pig brain SSADH (8). For ATP, binding with an estimated K_D of 4.3 mM was observed. Complete affinity titration was not possible for this lower affinity

interaction because the background at concentrations higher than 30 mM was too high. The maximum binding amplitude corresponded to a stoichiometry of 2 ATP molecules per SSADH tetramer. However, the additive binding amplitudes of NAD⁺ and ATP confirm the existence of a different binding site for ATP. Competitive binding of GTP to the ATP binding site was observed, but only ATP binding increased the dissociation constant of the NAD–*At*-SSADH1 complex. The consequence is an increased K_M and decreased V_{max} in the enzymes' kinetics.

From the binding data in this study and the previous kinetic data (5), we suggest that *At*-SSADH1 possesses two different nucleotide-binding sites. The site for the cofactor NAD⁺ binds also NADH and AMP in a competitive manner. Mass-sensitive detection by SPR revealed a second, low-affinity binding site, which seems to bind nucleotides with different effects on enzyme activity.

Only for ATP allosteric inhibition of NAD⁺ binding was observed by kinetic analysis (5) and by displacement assays. Analysis of the *At*-SSADH1 amino acid sequence for potential nucleotide binding sites revealed only one obvious candidate site, GSTAVGK, at position 245–251 of the mature protein (5). This motif perfectly matches the consensus sequence for the ATP-binding motif GxxxxGK[TS], also called the phosphate binding loop (P-loop) (11), but this phylogenetically conserved site in SSADH has already been implicated in NAD⁺/NADH binding (12–14). A second similar, but not identical motif, GLGREG, is present at residues 468–473 of the mature *At*-SSADH1. However, this site lacks the conserved lysine residue of the P-loop. Therefore, a second binding site for nucleotides to the *At*-SSADH1 monomer is not substantiated by sequence analysis. Another aspect that may underline the mechanism of ATP inhibition is the number of substrate molecules that bind to each tetrameric enzyme. Although each tetramer has four potential NAD⁺/NADH binding sites, analysis of the tetrameric SSADH from pig brain (8) suggested that only two molecules of NADH bind to the enzyme. If this is true also for the plant enzyme, as suggested by the preliminary stoichiometric data for NAD⁺ binding to immobilized ST-*At*-SSADH1, binding of ATP to the remaining unoccupied nucleotide-binding sites could well explain the noncompetitive effect of ATP. In this model, the *At*-SSADH1 tetramer possesses two high-affinity nucleotide binding sites, which bind NAD⁺, NADH, and AMP, and two low-affinity binding sites, which bind ATP and GTP. However, the exact stoichiometry for the binding of ATP per SSADH tetramer, as well as the precise K_D for ATP binding to *At*-SSADH1, needs to be determined to assess the validity of this model. Structural data from *At*-SSADH1 crystallized in the presence of different nucleotides may also provide important information in this regard.

Given the low affinity of ATP to *At*-SSADH1, the physiological relevance of ATP binding to *At*-SSADH1 depends on the concentrations of ATP and *At*-SSADH1 in mitochondria. ATP concentrations of several millimolar in mitochondria were reported (15). Moreover, low-affinity binding of nucleotides to proteins seems not to be unusual and was reported for the heat shock protein Hsp90, which binds ATP with a K_D in almost millimolar range (10). ATP is produced by oxidative phosphorylation in the respiratory

chain as well as by succinyl-Co-synthetase (SCS), which carries out the substrate level phosphorylation in the citric acid cycle and generates succinate alternatively to SSADH. Interestingly, succinyl-Co-synthetase in plants generates ATP, while in animals it generates GTP. Apparently the β -subunit of SCS determines the specificity (16). Here we show that SSADH activity from plants is affected by ATP, although it also binds GTP, probably at the same binding site.

Collectively, the data presented here support the model for the regulation of the last step of the GABA shunt by mitochondrial reducing potential and energy charge (5), consistent with accumulating evidence for the important role of the GABA shunt in plant metabolism (1, 2). The regulation of SSADH by ATP suggests a tight control of the rate of substrates provided by the GABA shunt to the respiratory chain. Consequently, the feedback regulation may also play a role in controlling the steady-state levels of GABA and, hence, possible functions of GABA via pathways other than the Krebs cycle.

In summary, we employed two techniques to investigate high- and low-affinity binding of nucleotides to plant SSADH. Mass-sensitive detection by SPR in combination with affinity capturing of the enzyme proved valuable for quantifying nucleotide–enzyme interactions. This method, with further optimization, has the potential to be used for studying binding of various nucleotides to different enzymes without the need to alter or label the nucleotide. In particular, for very sensitive redox enzymes, functional immobilization by affinity capturing may be the key for successful binding experiments. The immobilization method should be applicable to other recombinant enzymes, solely requiring the addition of the Strep-tag peptide to their coding sequence.

ACKNOWLEDGMENT

We thank Dr. Amnon Horovitz and Ariel Lindner for fruitful discussions and critical reading of the manuscript.

REFERENCES

- Shelp, B. J., Bown, A. W., and McLean, M. D. (1999) *Trends Plant Sci.* 4, 446–452.
- Baum, G., Lev-Yadun, S., Fridmann, Y., Arazi, T., Katsnelson, H., Zik, M., and Fromm, H. (1996) *EMBO J.* 15, 2988–2996.
- Snedden, W. A., Koutsia, N., Baum, G., and Fromm, H. (1996) *J. Biol. Chem.* 271, 4148–4153.
- Breitkreuz, K. E., and Shelp, B. J. (1995) *Plant Physiol.* 108, 99–102.
- Busch, K. B., and Fromm, H. (1999) *Plant Physiol.* 121, 589–597.
- Gonzales, M. P., Oset-Gasque, M. J., Gimenez Solves, A., and Canadas, S. (1987) *Comp. Biochem. Physiol.* 86, 489–492.
- Schmidt, T. G. M., Koepke, J., Frank, R., and Skerra, A. (1996) *J. Mol. Biol.* 255, 753–766.
- Blaner, W. S., and Churchich, J. E. (1980) *Eur. J. Biochem.* 109, 431–437.
- Hengsakul, M., and Cass, A. E. (1997) *J. Mol. Biol.* 266, 621–632.
- Scheibel, T., Neuhofen, S., Weikl, T., Mayr, C., Reinstein, J., Vogel, P. D., and Buchner, J. (1997) *J. Biol. Chem.* 272, 18608–18613.
- Saraste, M., Sibbald, P. R., and Wittinghofer, A. (1990) *Trends Biol. Sci.* 15, 430–434.

12. Hempel, J., Nicholas, H., and Lindahl, R. (1993) *Protein Sci.* 2, 1890–1900.
13. Chambliss, K. L., Caudle, D. L., Hinson, D. D., Moomav, C. R., Slaughter, C. A., Jacobs, C., and Gibson, K. M. (1995) *J. Biol. Chem.* 270, 461–467.
14. Vedadi, M., Vrielenk, A., and Meighen, E. (1997) *Biochem. Biophys. Res. Commun.* 238, 448–451.
15. Pradet, A., and Raymond, P. (1983) *Annu. Rev. Plant. Physiol.* 34, 199–224.
16. Johnson, J. D., Muhonen, W. W., and Lambeth, D. O. (1998) *J. Biol. Chem.* 273, 27573–27579.

BI000589E